World Academy of Science, Engineering and Technology
International Journal of Electrical and Computer Engineering
Vol:4, No:7, 2010

A Grid Current-controlled Inverter with Particle Swarm Optimization MPPT for PV Generators

Hanny H. Tumbelaka, and Masafumi Miyatake

***Abstract*—**This paper proposes a three-phase four-wire current-controlled Voltage Source Inverter (CC-VSI) for both power quality improvement and PV energy extraction. For power quality improvement, the CC-VSI works as a grid current-controlling shunt active power filter to compensate for harmonic and reactive power of loads. Then, the PV array is coupled to the DC bus of the CC-VSI and supplies active power to the grid. The MPPT controller employs the particle swarm optimization technique. The output of the MPPT controller is a DC voltage that determines the DC-bus voltage according to PV maximum power. The PSO method is simple and effective especially for a partially shaded PV array. From computer simulation results, it proves that grid currents are sinusoidal and in-phase with grid voltages, while the PV maximum active power is delivered to loads.

***Keywords*—**Active Power Filter, MPPT, PV Energy Conversion.

Open Science Index, Electrical and Computer Engineering Vol:4, No:7, 2010 publications.waset.org/1550/pdf

I. Introduction

IN AC-DC power conversion, a high-frequency switched power converter (inverter) is generally used to control the desired power flow between the AC side and the DC side. The basic popular type of a power converter is a Voltage Source Inverter (VSI) because it is easy to implement, low loss and low cost. Nowadays, power flow control in the VSI (especially for grid connected system) can be achieved using a current-control technique. By controlling the switching instants, the current-controlled VSI (CC-VSI) produces the desired current flow using instantaneous current feedback [1].

The DC side of the VSI is generally connected to a DC load or, in many applications, a power source such as batteries and photovoltaic panels. On the other hand, the AC side of the VSI is often an AC load or can be a voltage source from a grid, or a generator.

For applications, A CC-VSI can be used as a shunt active power filter (APF) to improve the power quality of the power system [2-4]. The CC-VSI operates to cancel the harmonics, as well as reactive power from the non-linear loads so that the grid currents will be sinusoidal with unity power factor. The AC side of the CC-VSI connects to the AC grid at the point of common coupling (PCC) and parallel to the loads, while the DC bus of the CC-VSI contains a DC capacitor. A CC-VSI can also be applied to transfer active power from a DC source such as a battery or a renewable energy source to the AC grid (grid-connected system), as well as to loads.

Hanny H. Tumbelaka is with the Department of Electrical Engineering, Petra Christian University, Surabaya, Indonesia. e-mail: tumbeh@petra.ac.id
Masafumi Miyatake is with the Department of Engineering and Applied Sciences, Sophia University, Tokyo, Japan. e-mail: miyatake@sophia.ac.jp

If connected to a renewable energy source such as solar cells, it is also expected that the VSI has the ability to extract the maximum power from the PV panels. In literatures [5-7], the power converter operates as a single-stage circuit to achieve directly DC-AC energy transfer with maximum power point tracking (MPPT).

Since the CC-VSI for transferring active power and for canceling harmonics has a similar configuration, it is potential to integrate both functions in one CC-VSI. In this way, the power converter would be able to improve the system power quality as well as to deliver energy from renewable energy sources.

There are few literatures that discuss about combining PV power extraction and active filtering such as in [8-9]. Literature [8] requires calculation of load active power and PV output power to determine the inverter current. Due to switching device safety, power flow of PV power is processed first, while power quality improvement is in the second priority. Moreover, DC-bus controller is used during no insolation. In [9], the current controller requires the measurement of both the load and the inverter currents. The load current is used to calculate the reactive- and harmonic-rich reference value for the inverter current that could create errors and time delays.

This paper proposes a simple and integrated method for a grid connected CC-VSI to supply extracted power from PV panels to the grid/load as well as to mitigate and regulate the harmonic and reactive power injected into the utility grid. In addition, the MPPT controller used in this paper is particle swarm optimization (PSO) technique that is suitable for the PV system with partially shaded. The effectiveness of the MPPT controller and its compatibility with the CC-VSI controller will also be explained.

II. The CC-VSI

The three-phase four-wire CC-VSI for active filter and PV energy extraction is a three-phase bridge inverter with a common DC bus. The bridge inverter contains six IGBTs with anti-parallel diodes. There are inductors at the AC side and a mid-point earthed split capacitor at the DC-bus. The control system consists of a current control loop to control the harmonic and reactive power and a voltage control loop to control the active power [3-4]. The speed of response of the voltage control loop is much slower than that of the current control loop. Hence, the current control loop and voltage control loop are decoupled. Moreover, there is a PV array supported by a MPPT controller is coupled to the DC-bus of the CC-VSI. Fig. 1 shows the proposed CC-VSI configuration.

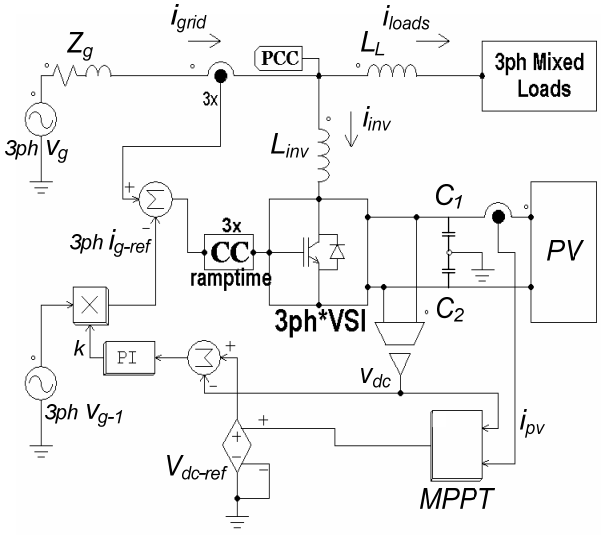


Fig. 1. The proposed CC-VSI configuration

A. Current Control Loop

The current control loop shapes the grid currents, rather than VSI currents, to be sinusoidal and in-phase with the grid voltages by generating a certain pattern of bipolar PWM for continuous switching of the power converter switches according to a ramptime current control technique.

The ramptime current control (RCC) technique has been established as described in the literature [1][12][13]. The principle operation of RCC is similar to a sliding mode control and based on the concept of zero average current error (ZACE). The current error signal is forced to have an average value equal to zero with a constant switching frequency. The RCC maintains the area of positive current error signal excursions (A+) equal to the area of negative current error signal excursions (A−), resulting in the average value of the current error signal being zero over a switching period (Fig. 2). The switching period (or frequency) is also kept constant based on the choice of switching instants relative to the zero crossing times of the current error signal. The RCC has a high bandwidth with a fast transient response that can quickly follow the rapid changes in non linear loads.

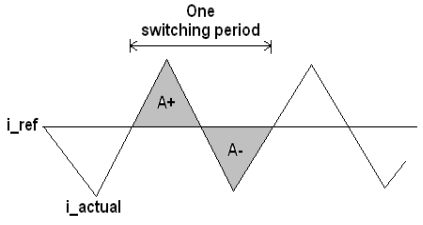


Fig. 2: Zero average current error (ZACE)

In this case, the current sensors are located on the grid side. The grid currents are sensed and directly controlled to follow symmetrical sinusoidal reference signals ($i_{g\text{-}ref}$), which is in-phase with the grid voltages. The reference signal waveform is the same as the fundamental component of the grid voltage, which is obtained using a PLL circuit. The outputs of the sensors are compared to the reference signals to generate current error signals. The current error signals, which are the difference between the actual currents (grid currents – i_{grid}) and the reference signals – $i_{g\text{-}ref}$, are processed using ramptime current control to generate PWM signals for driving the power switches. Hence, by forcing the grid currents to be identical to the reference signals, the CC-VSI operates as a shunt active power filter (APF) and automatically provides the harmonic, reactive, negative- and zero-sequence currents for the load according to the basic current summation rule (1) without measuring and determining the unwanted load current components.

$$i_{grid} = i_{inv} + i_{loads} \quad (1)$$

B. Voltage Control Loop

The voltage control loop contains a simple Proportional Integral (PI) control to maintain the DC-bus voltage at the reference voltage level ($V_{dc\text{-}ref}$). In this case, the DC-bus voltage is sensed and directly controlled to follow $V_{dc\text{-}ref}$. The voltage control loop also provides the amplitude of grid currents as well as maintains the active power balanced among the grid, the load and the VSI.

If active power unbalance occurs in the system, there is a voltage deviation (ΔV_{dc}) in the DC bus relative to the reference voltage. For perfect tracking in the current control loop, the voltage control loop responds to adjust the amplitude of grid currents appropriately by adjusting the amplitude of $i_{g\text{-}ref}$ as well as to recover the DC-bus voltage to the reference voltage level. The output of the PI controller, which is a gain k, can determine the amount of ΔV_{dc} that corresponds to the grid current amplitude. The average DC-bus voltage is then recovered and stays at the reference voltage. New steady state active power balance has been achieved with new grid current amplitude. The sinusoidal grid current reference signal is given by

$$i_{g\text{-}ref} = k\, v_{g\text{-}1} \quad (2)$$

where $v_{g\text{-}1}$ is the fundamental component of the grid voltage obtained from a PLL circuit. The value of k is the output of the PI controller. This is an effective way of determining the required magnitude of the grid current, since any mismatch between the required load active power and that being forced by the CC-VSI would result in the necessary corrections to regulate the DC-bus voltage.

III. PV Energy Extraction

The CC-VSI configuration in Fig. 1 has a capability to deliver the solar energy to the AC grid. PV arrays are coupled to the DC bus and parallel to DC-bus capacitors (C_1 and C_2). The amount of active power injected from PV panels is determined by the PV output voltage, which is equal to the DC bus voltage (v_{dc}). For PV array with 1 parallel string and 25 series modules per string, the *p-v* curve of Fuji Electric PV modules (ELR-615-160Z) for several levels of irradiance is shown in Fig. 3. The fluctuation of solar irradiation leads to the variation of PV output power.

Open Science Index, Electrical and Computer Engineering Vol:4, No:7, 2010 publications.waset.org/1550/pdf

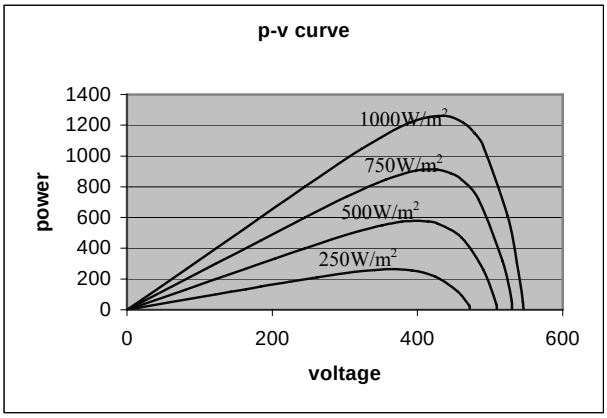


Fig. 3. *p-v* curves of the PV array

The PV modules have to be arranged in an array such that the PV output voltage has to be greater than twice of the peak value of the grid voltage [10]. Otherwise, the CC-VSI is unstable and unable to deliver currents to the grid. On the other hand, there is an upper limit to satisfy voltage insulation requirements of power electronic components.

In addition, there is a MPPT control circuit as a part of the PV system. The output of the MPPT controller sets up the DC-bus reference voltage ($V_{dc\text{-}ref}$) corresponding to the PV maximum power. The inputs of the MPPT controller are the output voltage and current of the PV panels. As mentioned before, the voltage control loop will maintain the DC-bus voltage at the reference voltage level. If the DC-bus voltage reaches the reference voltage, the PV output power will be at maximum. At the same time, the active power balance among the grid, the load and the PV panels connected to the DC-bus occurs. The active power of the loads is supplied from the grid and the PV maximum power injection. Thus, the MPPT controller is independent on the current control loop and the voltage control loop of the CC-VSI because it works outside both control loops and simply focuses on setting up the DC-bus reference voltage. The fluctuation of solar irradiation leads to the variation of the DC-bus reference voltage to obtain the PV maximum power.

IV. Particle Swarm Optimization (PSO) MPPT [11]

A PSO method uses several cooperative agents (Fig. 4). Each agent shares the obtained information during the searching process. Moreover, each agent moves in the search space with a velocity (x_i^k) according to its own previous best information (solution) and its group's previous best solution. The velocity as well as the position (s_i^k) of agents will be updated as

$$x_i^{k+1} = w x_i^k + c_1 r_1 (p_{best-i} - s_i^k) + c_2 r_2 (g_{best} - s_i^k) \quad (3)$$

$$s_i^{k+1} = s_i^k + x_i^{k+1} \quad (4)$$

where w is the momentum factor; c_1 and c_2 are positive constant; r_1 and r_2 are the random numbers and their values are in between (0–1). The variable $p_{best\text{-}i}$ is used to memorize the best position that the i^{th} agent has found so far. It is updated as (5) if the condition (6) is satisfied. The variable g_{best} is used to store the best position achieved among all agents.

$$p_{best-i} = s_i^k \quad (5)$$

$$f(s_i^k) > f(p_{best-i}) \quad (6)$$

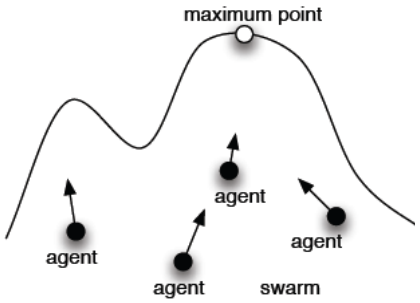


Fig. 4. Searching process

A. Application of PSO to MPPT controller

For a MPPT controller, the agent position (as well as p_{best} and g_{best}) means the PV output voltage, which is equal to the DC-bus voltage. The objective function $f(s_i^k)$ can be considered as the PV output power that would be maximized.

Application of the tracking process to the circuit shown in Fig. 1 will be generally as follows:

1. Set initial conditions of agents. Each agent has its own initial position (voltage), velocity and objective function (power).
2. Each agent voltage determines the DC-bus reference voltage ($V_{dc\text{-}ref}$). If the DC-bus voltage is equal to $V_{dc\text{-}ref}$ due to the voltage control loop, then measure the PV output power, which is stored as agent power. Each agent has its own power corresponding to its voltage.
3. Each agent voltage searches for p_{best} by comparing its power $f(s_i^k)$ and $f(p_{best-i})$, whether $f(s_i^k) > f(p_{best-i})$ or $f(s_i^k) < f(p_{best-i})$.
4. Find g_{best} from all agent p_{best} by comparing all agent p_{best} power.
5. Each agent moves with a velocity x_i^{k+1}. The velocity of agent equals to zero when the agent reaches MPP in steady state.
6. Each agent has a new voltage s_i^{k+1}
7. Return to 2 with each agent's new voltage

As mentioned before, the DC-bus voltage range is limited due to system stability and device insulation requirements, which is in this case in between 370V (V_{min}) and 470V (V_{max}). Outside the limits, the PSO will not be able to find the MPP.

The PV array generates two or more maximum power points (MPPs) if the PV array is partially shaded by the

Open Science Index, Electrical and Computer Engineering Vol:4, No:7, 2010 publications.waset.org/1550/pdf

shadow of building, tree, etc. Fig. 5 demonstrates that the current generated by the shaded module is less than the fully illuminated module. As a result, two MPPs exist. In the PV array, those modules are connected in series. Thus, the current flowing through the modules is the same. Under this condition, the excess current flows through a by-pass diode. It is not difficult for the PSO to find the global maximum point for the system having many local optimal points. Agents will move to search for g_{best}.

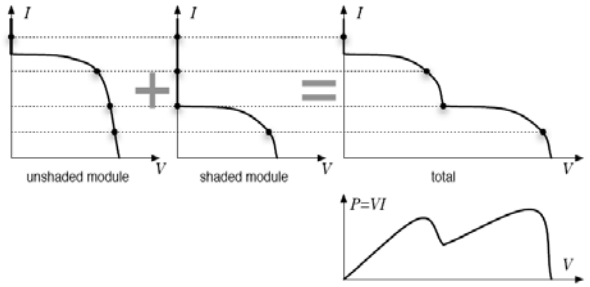


Fig. 5. PV partially shaded

V. Simulation Results

The system shown in Fig. 1 is examined using computer simulation (PSIM®) to verify the concepts. Table 1 describes the parameter values for the system. The three-phase grid voltages contain harmonics (THD_V = 3.9%), and the mixed loads consist of single- and three-phase linear and non-linear loads as shown in Fig. 6. The characteristics of the PV modules have been represented in Fig. 3. For the PSO MPPT, the number of agents is three (i = 1,2,3), and the parameter values of $w = 0.4$, $c_1 = 1.3$, $c_2 = 1.7$.

TABLE 1
PARAMETER VALUES FOR THE SYSTEM UNDER STUDY

Symbol	Description	Value
v_g	AC grid voltage, line-line, *rms*	207 V
F	AC line/grid frequency	50 Hz
L_L	Series inductor	0.92 mH
V_{dc}	DC-bus voltage (minimum)	370 V
$C_1 = C_2$	DC Capacitors, electrolytic type	4000 μF
L_{inv}	Inverter inductor	1.52 mH
f_{sw}	Target switching frequency	15.6 kHz

The PV output voltage, which equals to the DC-bus voltage and PV output power in steady state are shown in Fig. 7 for insolation of 0.8kW/m2. As soon as the searching process starts, the agents search for p_{best} and g_{best}. The searching process continues by revising the agent voltages according to their velocity. The system converges when their velocity comes to zero. It can be seen that in steady state the PV output voltage as well as its maximum power matches to the insolation level.

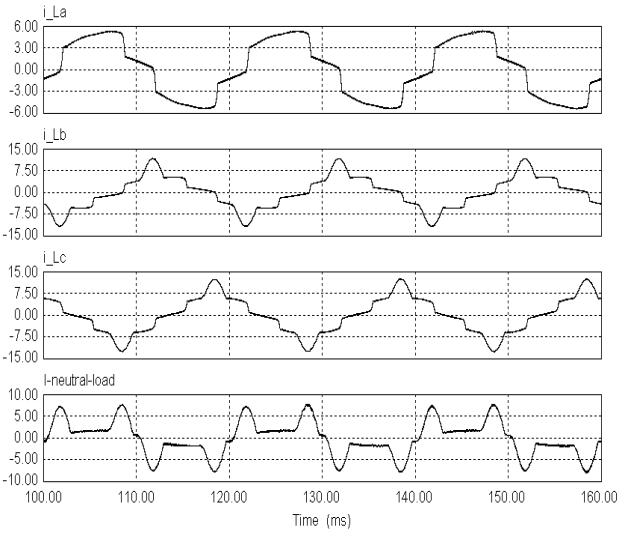


Fig. 6. Mixed-load currents (phase a-b-c-neutral)

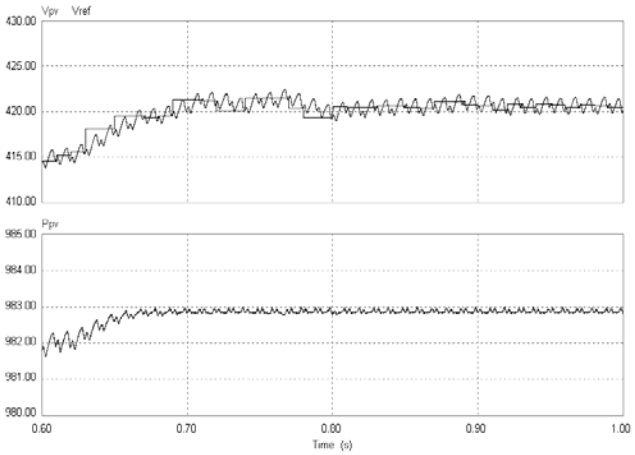


Fig. 7. PV output voltage and its reference (square wave) (top); PV output power (bottom)

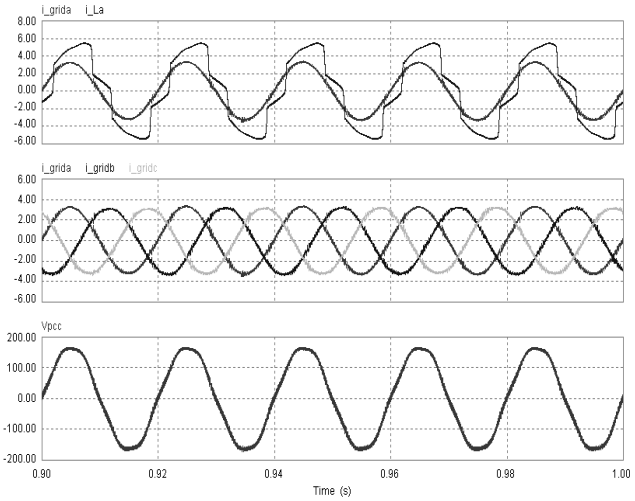


Fig. 8. (top to bottom) the grid (sinusoidal) and the load (non-sinusoidal) currents (phase A); three-phase grid currents; the grid voltage (phase A)

Open Science Index, Electrical and Computer Engineering Vol:4, No:7, 2010 publications.waset.org/1550/pdf

Fig. 8 illustrates the load current and grid current of phase A. It is obvious that the grid current is smaller than the load current, because the load is supplied by the grid and the maximum power extracted from the PV array. The grid currents are also sinusoidal, balanced and in-phase with the grid voltage due to active filtering operation.

When the irradiation level is below 0.3kW/m^2, the DC-bus voltage is clamped to 370V. Otherwise the system will be unstable. As a result, the MPPT controller is unable to operate for the PV maximum power extraction. Fig. 9 demonstrates that under insolation level of 0.1kW/m^2, the PV array supplies small power but not at maximum. At steady state, the PV output voltage is 370V.

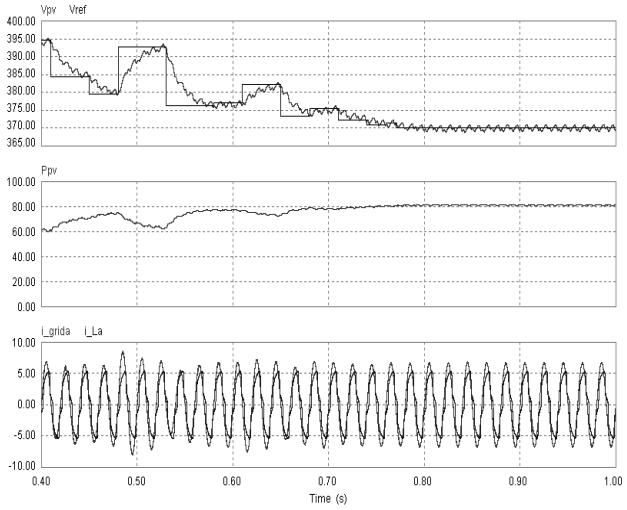


Fig. 9. Irradiation of 0.1kW/m^2 (top to bottom): PV output voltage (and its reference – square wave); PV output power; the grid and the load currents (phase A)

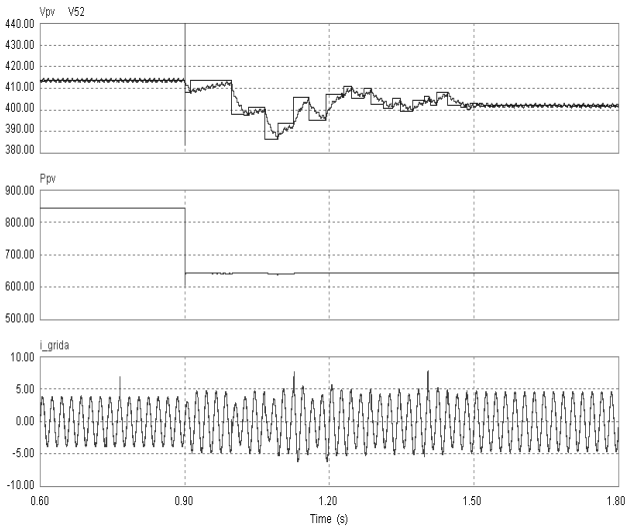


Fig. 10. When the insolation is changed (0.7kW/m^2 to 0.55kW/m^2) (top to bottom): PV output voltage (and its reference – square wave); PV output power; the grid current (phase A)

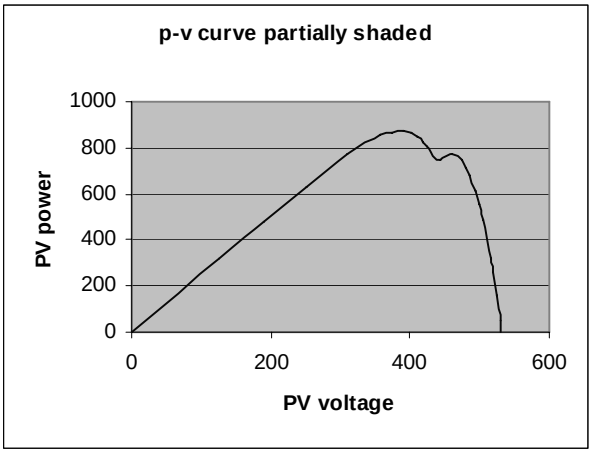


Fig. 11. *p-v* curve of PV array under partially shaded

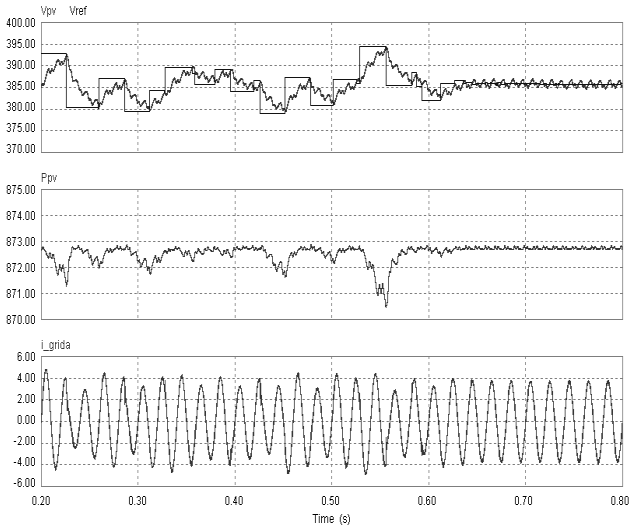


Fig. 12. PV array under partially shaded (top to bottom): PV output voltage (and its reference – square wave); PV output power; the grid current (phase A)

Fig. 10 shows the PV output voltage and power as well as the grid current when the irradiance is changed. The MPPT controller responds quickly and properly by revising each agent voltage as well as its velocity and searching the new g_{best} value for the new MPP.

Fig. 11 and 12 describe the behavior of the PV array in the section III under partially shaded. The *p-v* curve of such condition is shown in Fig. 11. It can be seen that there are two local maximum power points. One point is higher than another. Fig. 12 shows that the final result of the searching process is correct and the global maximum point (the highest point) is attained (PV output power reaches around 873W).

VI. Conclusion

This paper explains the capability of a grid connected CC-VSI for PV energy extraction and active filtering. It is obvious that both power quality improvement and PV energy extraction can be integrated easily using the grid current-controlled VSI. The control strategy using the current control

Open Science Index, Electrical and Computer Engineering Vol:4, No:7, 2010 publications.waset.org/1550/pdf

loop and the voltage control loop can handle both functions simultaneously. The current control loop directly shapes the grid currents to be sinusoidal and in-phase with the grid voltages, while the voltage control loop regulates the active power balance among the grid, the load and the power converter supported by PV panels. Those two control loops are able to compensate for the reactive and harmonic power as well as to manage the active power. At the same time the PSO MPPT controller searches independently for the PV maximum power. The PSO method is simple and effective to be applied to the PV system especially having many local maximum power points.

From simulation results, in steady state and dynamic condition, it proves that the system works very well. The CC-VSI supported by the PSO MPPT controller can perform as a shunt active power filter as well as a PV energy extractor.

REFERENCES

[1] Borle, L., *Zero Average Current Error Control Methods for Bidirectional AC-DC Converters*, PhD Thesis, 1999, Electrical and Computer Engineering, Curtin University of Technology, Western Australia

[2] El-Habrouk, M., M.K. Darwish, and P. Mehta, *Active power filters: a review*. Electric Power Applications, IEE Proceedings-, 2000. **147**(5): p. 403-413.

[3] Tumbelaka, H.H., L.J. Borle, and C.V. Nayar. *Analysis of a Series Inductance Implementation on a Three-phase Shunt Active Power Filter for Various Types of Non-linear Loads*. Australian Journal of Electrical and Electronics Engineering, Engineers Australia, 2005. **2**(3): p. 223-232.

[4] Tumbelaka, H.H., L.J. Borle, C.V. Nayar, and S.R.Lee, "A Grid Current-controlling Shunt Active Power Filter", *Journal of Power Electronics*, vol. 9, no. 3, 2009, p. 365-376.

[5] Chen, Y., and Smedley, K.M., *A Cost-Effective Single-State Inverter with Maximum Power Point Tracking*, IEEE Transactions on Power Electronics, 2004, 19(5): p. 1289-1294.

[6] Castaner, L., and Silvestre, S., *Modelling Photovoltaic System using PSpice*, John Wiley & Sons, 2002.

[7] Wanzeller, M.G. et.al., *Current Control Loop for Tracking of Maximum Power Point Supplied for Photovoltaic Array*, IEEE Transactions on Instrumentation and Measurement, 2004, 53(4): p. 1304-1310.

[8] Wu, Tsai-Fu et.al., *PV Power Injection and Active Power Filtering with Amplitude-Clamping and Amplitude-Scaling Algorithms*, IEEE Transactions on Industry Application, 2007, **43**(3): p.731-741

[9] Grandi, G., Casadei, D., and Rossi, C., Direct Coupling of Power Active Filters with Photovoltaic Generation System with Improved MPPT Capability, in IEEE Power Tech Conference, 2003. Bologna, Italy.

[10] Tumbelaka, H.H., L.J. Borle, and C.V. Nayar. *A New Approach to Stability Limit Analysis of A Shunt Active Power Filter with Mixed Non-linear Loads*. in Australasian Universities Power Engineering Conference (AUPEC). 2004. Brisbane, Australia: ACPE. p. ID: 121

[11] Miyatake, M. et al., *A Novel Maximum Power Point Tracker Controlling Several Converters Connected to Photovoltaic Arrays with Particle Swarm Optimization Technique*, in EPE-PEMC, 2007, Aalborg.

[12] L. J. Borle, and C. V. Nayar, "Ramptime Current Control", *in Conf. Proc. 1996 IEEE Applied Power Electronics Conference (APEC'96)*, p. 828-834.

[13] L. J. Borle, and C. V. Nayar, "Zero Average Current Error Controlled Power Flow for AC-DC Power Converter", *IEEE Trans. on Power Electronics*, **10**(1): pp. 725-732. 1995.

Open Science Index, Electrical and Computer Engineering Vol:4, No:7, 2010 publications.waset.org/1550/pdf